Robotica (2010) volume 28, pp. 359–368. © Cambridge University Press 2009
doi:10.1017/S0263574709005682

Experimental identification of the dynamics model for 6-DOF parallel manipulators

Houssem Abdellatif * and Bodo Heimann

Institute of Mechatronic Systems (former Institute of Robotics), Appelstr. 11, D-30167 Hannover, Germany

(Received in Final Form: April 9, 2009. First published online: May 22, 2009)

SUMMARY

The paper presents a self-contained approach for the dynamics identification of six degrees of freedom (DOF) parallel robots. Major feature is the consequent consideration of structural properties of such machines to provide an experimentally adequate identification method. The known periodic excitation is modified and enhanced to take the actuator coupling as well as the numerical solution of the direct kinematics into account. The benefits of explicit frequency-domain data filtering are demonstrated. Additionally, a new implementation of the maximum-likelihood estimator allows for automatic tuning of the data filter. The issue of optimal input experiment design is also discussed and substantiated with extensive experiments.

KEYWORDS: Parallel manipulators; Dynamics; Identification; Optimal experiment design.

1. Introduction

It is well known that model-based controller and simulation environments perform as well, as a reliable estimation of model parameters is available. In the last two decades an impressive progression has been achieved, concerning the dynamics identification of open-chain robotic manipulators. The expression of the dynamics in parameter linear form, the use of linear estimation techniques and the appropriate design of excitation trajectories became standard procedures and state of the art.[1–5]

The portability of the research progress is, however, not yet achieved on the recently emerging class of closed-loop and parallel kinematic manipulators (PKM). The important structural and architectural variety of such robots complicates the task. To our opinion and concerning the identification of dynamics models, two main categories can be addressed: lower mobility and higher mobility PKM. The first have at most one rotational degree of freedom (DOF) for the endeffector, whereas their counterpart, the higher mobility robots possess at least two rotational DOFs. For lower mobility PKM and in the majority of cases, the actuated (or articulated) variables are sufficient to determine the manipulator's configuration. They coincide with the set of generalized coordinates. Consequently, the dynamics and therefore the regressor of the estimation can be directly expressed with respect to the measurable actuated joint variables. From the identification point of view there is no significant difference between serial robots and lower mobility PKM. This has been demonstrated by some recent publications.[6–9] The situation is not that favorable for higher mobility robots, i.e., for 6-DOF parallel manipulators. In such case the actuated variables are not independent and yields ambiguous solution of the direct kinematics.[10] In that sense the generalized coordinates are chosen to be the pose of the endeffector, which is usually not measurable and has to be calculated numerically from the actuation variables.[11] As a result, the estimation regressor has to be built up using nonmeasured variables that are corrupted additionally to noise by numerical imprecisions. By considering the classic case of 6-DOF parallel robot, i.e., the famous Stewart–Gough platform, so it is interesting to state the missing of systematic identification methodologies in the literature, despite all the progress made in dynamics identification.

This paper addresses the subject of dynamics identification for 6-DOF nonredundant parallel manipulators. The presented approach exploits the progress of the established identification theory to provide an experimentally adequate and appropriate method for the investigated class of dynamic systems. Therefore, the paper emphasizes on the practical issues and the experimental proceeding. It is the goal to provide the interested reader with the hints for a successful dynamics identification of 6-DOF PKM, since accurate dynamics identification is highly crucial for the improvement of control performance of such machines.[12]

Beyond the recall of some basics on robot dynamics and estimation theory, which we have published in refs. [13–15], the paper illustrates the subject of appropriate signal processing for the dynamics identification of spatial parallel robots. A novel discussion is given that considers the relationship between data filtering and the use of the numerical direct kinematics that provides the state coordinates of parallel robots. By proposing strict frequency-domain data processing, a novel formulation of the maximum-likelihood estimation can be derived. This new formulation increases the parameter set to be identified by a single new value that corresponds to the cutoff-frequency of the data filter. In such manner, a considerable computational efficiency is achieved, compared to already established approaches in the literature.[5,16]

The paper is structured such that some discussion and experimental examples are provided within algorithmic development. In such manner, the reader is provided with

* Corresponding author. E-mail: houssem.abdellatif@imes.uni-hannover.de

a substantiated motivation of the ideas behind the proposed proceeding. Section 2 gives a brief review on identification approaches well-known in robotics. Additionally, the dynamics model of parallel robots is revisited. We focus on the form that is necessary for linear identification, namely the linear-in-the-parameter (LP) form. It is recalled that the model is given analytically only at the level of generalized forces. The actuation forces and the estimation regressor are calculated by using the manipulator's Jacobian. The latter is obtained numerically, such that gradient-based maximum-likelihood estimators—as proposed in ref. [16]—are not useful.

In Section 3 follows the adaptation of the powerful approach of periodic excitation trajectories proposed by Swevers *et al.*[5] to 6-DOF PKM. For such systems the issue of data processing and filtering plays a central role for the experimental success of the identification. For example, the use of numerical direct kinematics yields a spectral distortion in the calculated data, such that the filtering method given by refs. [5, 16] will lead to leakage effects. Thus, a strict frequency domain data processing is proposed. The approach passes on the exact knowledge of the excitation frequencies. Furthermore, the high coupling between the actuators does not allow for SISO disturbance models, like it is often done in the case of serial robots.[3,5,17] The additional consideration of cross-correlated data is suggested. The estimated covariances are useful for accurate identification and also for the optimal input design of the experiments and helps to overcome the classic excitation design paradigm that uses the condition number of the regressor.[4,7,6] The new approach for implementing the maximum-likelihood estimator for parallel robots is discussed in Section 5.

The last Section 6 is dedicated the experiments. The proposed methodology is substantiated on the directly driven hexapod PaLiDA (see Fig. 3). The effects of filtering and experiment design on the accuracy of the identified models, as well as on the improvement of tracking control are demonstrated by means of experimental results.

2. Identification of Dynamics Models for Parallel Robots

The use of linear estimators in robotics is widely spread, since the dynamics equations can be written in a linear form with respect to model base parameters. For all robot classes this can be obtained as follows

$$\boldsymbol{\tau} = \boldsymbol{A}(\boldsymbol{z}, \dot{\boldsymbol{s}}, \ddot{\boldsymbol{s}})\boldsymbol{p}, \tag{1}$$

with the model output being the generalized forces $\boldsymbol{\tau}$, the model input being the generalized coordinates $\boldsymbol{z}$, velocities $\dot{\boldsymbol{s}}$ and accelerations $\ddot{\boldsymbol{s}}$, and the parameter vector $\boldsymbol{p}$ regrouping a base set of rigid-body and friction parameters.[3] The case is favorable for serial robot manipulators, since all inputs and outputs correspond to the actuation space. Furthermore, Eq. (1) is obtained analytically and in a closed form.[3,5] The situation changes for the case of higher mobility PKM, where the configuration space, the actuation space and the joint space are all different.[12] The parameter linear closed form is obtained for the rigid-body dynamics with respect to the configuration space:

$$\boldsymbol{\tau}_{\mathrm{rb}} = \boldsymbol{A}_{\mathrm{rb}}(\boldsymbol{x}, \boldsymbol{v}, \boldsymbol{a})\boldsymbol{p}_{\mathrm{rb}}, \tag{2}$$

where $\boldsymbol{z}$, $\dot{\boldsymbol{s}}$, and $\ddot{\boldsymbol{s}}$ have been set to be the pose $\boldsymbol{x}$, the velocity $\boldsymbol{v}$ and the acceleration $\boldsymbol{a}$ of the endeffector, respectively. The friction dynamics are obtained with respect to the joint space

$$\boldsymbol{Q}_{\mathrm{f}} = \boldsymbol{A}_{\mathrm{f}}(\dot{\boldsymbol{q}})\boldsymbol{p}_{\mathrm{f}}, \tag{3}$$

with $\boldsymbol{q}$ denoting all joint variables including the passive $\boldsymbol{q}_{\mathrm{p}}$ and the active ones $\boldsymbol{q}_{\mathrm{a}}$. From the estimation point of view Eqs. (2) and (3) consist in models that are linear with respect to their parameters (subsequently abbreviated LP models) but with different input spaces. For a uniform formalism Eq. (3) can be rewritten in

$$\boldsymbol{Q}_{\mathrm{f}} = \boldsymbol{A}_{\mathrm{f}}(\boldsymbol{x}, \boldsymbol{v})\boldsymbol{p}_{\mathrm{f}}, \tag{4}$$

which is possible since all joint variables and velocities $\dot{\boldsymbol{q}}$ can be directly obtained in a closed form by means of the inverse kinematics.[10] Because both $\boldsymbol{\tau}$ and $\boldsymbol{Q}_{\mathrm{f}}$ are not measurable, the former equations need to be transformed with respect to the actuation space, where at least the output of the final model is measurable. We obtain for the rigid-body dynamics

$$\begin{aligned}\boldsymbol{Q}_{\mathrm{a,rb}} &= \left(\frac{\partial \boldsymbol{v}}{\partial \dot{\boldsymbol{q}}_{\mathrm{a}}}\right)^{\mathrm{T}} \boldsymbol{A}_{\mathrm{rb}}(\boldsymbol{x}, \boldsymbol{v}, \boldsymbol{a})\boldsymbol{p}_{\mathrm{rb}}, \\ &= \boldsymbol{J}^{\mathrm{T}}\boldsymbol{A}_{\mathrm{rb}}(\boldsymbol{x}, \boldsymbol{v}, \boldsymbol{a})\boldsymbol{p}_{\mathrm{rb}},\end{aligned} \tag{5}$$

and for friction

$$\begin{aligned}\boldsymbol{Q}_{\mathrm{a,f}} &= \left(\frac{\partial \dot{\boldsymbol{q}}}{\partial \dot{\boldsymbol{q}}_{\mathrm{a}}}\right)^{\mathrm{T}} \boldsymbol{A}_{\mathrm{f}}(\boldsymbol{x}, \boldsymbol{v})\boldsymbol{p}_{\mathrm{f}}, \\ &= \left(\frac{\partial \dot{\boldsymbol{q}}}{\partial \boldsymbol{v}}\frac{\partial \boldsymbol{v}}{\partial \dot{\boldsymbol{q}}_{\mathrm{a}}}\right)^{\mathrm{T}} \boldsymbol{A}_{\mathrm{f}}(\boldsymbol{x}, \boldsymbol{v})\boldsymbol{p}_{\mathrm{f}}, \\ &= \boldsymbol{J}^{\mathrm{T}}\boldsymbol{J}_L^{\mathrm{T}}\boldsymbol{A}_{\mathrm{f}}(\boldsymbol{x}, \boldsymbol{v})\boldsymbol{p}_{\mathrm{f}}.\end{aligned} \tag{6}$$

For 6-DOF parallel robots, the jacobian of the manipulator $\boldsymbol{J}$ is not available analytically and has to be obtained by numerical inversion[10] of $\boldsymbol{J}^{-1}$. This means that the final linear form of the dynamics, which relates the input to the output is not available in a closed form due to the presence of $\boldsymbol{J}$

$$\boldsymbol{Q}_{\mathrm{a}} = \underbrace{\boldsymbol{J}^{\mathrm{T}}\begin{bmatrix}\boldsymbol{A}_{\mathrm{rb}} & \boldsymbol{0} \\ \boldsymbol{0} & \boldsymbol{J}_L\boldsymbol{A}_{\mathrm{f}}\end{bmatrix}}_{\boldsymbol{A}}\underbrace{\begin{bmatrix}\boldsymbol{p}_{\mathrm{rb}} \\ \boldsymbol{p}_{\mathrm{f}}\end{bmatrix}}_{\boldsymbol{p}} = \boldsymbol{A}(\boldsymbol{x}, \boldsymbol{v}, \boldsymbol{a})\,\boldsymbol{p}. \tag{7}$$

By considering N noisy measurements at N configurations, the formulation of the estimation problem can be derived from Eq. (7) as

$$\underbrace{\begin{bmatrix}\boldsymbol{Q}_{\mathrm{a}_1} \\ \vdots \\ \boldsymbol{Q}_{\mathrm{a}_N}\end{bmatrix}}_{\boldsymbol{\Gamma}} = \underbrace{\begin{bmatrix}\boldsymbol{A}(\boldsymbol{x}_1, \boldsymbol{v}_1, \boldsymbol{a}_1) \\ \vdots \\ \boldsymbol{A}(\boldsymbol{x}_N, \boldsymbol{v}_N, \boldsymbol{a}_N)\end{bmatrix}}_{\boldsymbol{\Psi}}\boldsymbol{p} + \underbrace{\begin{bmatrix}\boldsymbol{e}_1 \\ \vdots \\ \boldsymbol{e}_N\end{bmatrix}}_{\boldsymbol{\eta}}, \tag{8}$$

https://doi.org/10.1017/S0263574709005682 Published online by Cambridge University Press

with the measurement vector $\mathbf{\Gamma}$, the information or regression matrix $\mathbf{\Psi}$ and the error vector $\boldsymbol{\eta}$ that accounts for output additive disturbances. By assuming the disturbance $\boldsymbol{\eta}$ to be gaussian with zero-mean the Gauss–Markov (GM) approach yields the best unbiased solution

$$\hat{\boldsymbol{p}}_{GM} = \left(\mathbf{\Psi}^{\mathrm{T}}\mathbf{\Sigma}_{\eta\eta}^{-1}\mathbf{\Psi}\right)^{-1}\mathbf{\Psi}^{\mathrm{T}}\mathbf{\Sigma}_{\eta\eta}^{-1}\mathbf{\Gamma}, \tag{9}$$

of the overdetermined linear equations system, Eq. (8).[18,19] Here $\mathbf{\Sigma}_{\eta\eta} = \mathbf{E}(\boldsymbol{\eta}\boldsymbol{\eta}^{\mathrm{T}})$ is the covariance of the disturbance vector $\boldsymbol{\eta}$. The application of the linear techniques assumes not only a linear observation model but it assumes also output additive noise, which means noise-free or at least noise-poor regressor $\mathbf{\Psi}$. When such condition is not fulfilled, the maximum-likelihood estimator should be adopted (see Section 5).

The regressor is built up using $\boldsymbol{x}$, $\boldsymbol{v}$, and $\boldsymbol{a}$ which are not directly measured. Numerical direct kinematic algorithms can be used to calculate the pose from the measured actuated variables $\boldsymbol{q}_{\mathrm{a}}$.[11,20] The use of the Newton–Raphson algorithm, e.g., is here recommended, since it is performed offline. Hence, it is not critical to achieve appropriate choice of the initial values and algorithm resolution. More critical is the calculation of $\boldsymbol{v}$ and $\boldsymbol{a}$. Numerical differentiation is not convenient, because possible oscillations of the direct kinematic solution introduce additional noise, even in the case of highly accurate actuator measurements.[13] Appropriate methods for the reconstruction of the velocities and acceleration are proposed in the following (see Section 3). The direct dependency of the regressor $\mathbf{\Psi}$ on $\boldsymbol{x}$, $\boldsymbol{v}$, and $\boldsymbol{a}$ demands a planning of the excitation or identification trajectories with respect to the workspace that is for parallel manipulators equal to the configuration space.

Another interesting issue with 6-DOF parallel robots is the presence of passive joints that produce additional but nonmeasurable friction forces. The detection of all friction forces could be achieved only indirectly by using appropriate kinematic coupling models and actuation forces.[21] Since in addition the number of passive joints exceeds that of the actuators, it is plausible to ask, whether all joint effects can be significantly detected in the noisy measurements of actuator forces. Optimal parameter number and identifiable structures should be investigated before starting the identification. The determination of identifiable minimal parameter for rigid-body dynamics is a standard procedure.[4,15,22,] For friction model no uniform or standard approach is known in the literature yet. In a previous paper,[1]4 we proposed the following a methodology that is based on the estimation uncertainty. The covariance $\boldsymbol{P}$ of the GM parameter estimate is given for the LP model structure Eq. (7) and by ref. [19]:

$$\boldsymbol{P}(\hat{\boldsymbol{p}} = \hat{\boldsymbol{p}}_{GM}) = \left(\mathbf{\Psi}^{\mathrm{T}}\mathbf{E}^{-1}(\boldsymbol{\eta}\boldsymbol{\eta}^{\mathrm{T}})\mathbf{\Psi}\right)^{-1}. \tag{10}$$

The asymptotical distribution of the ith model parameter is a expected to be normal with the variance $\sigma_{p_i}^2$ that is equal to the ith diagonal entry of the covariance matrix P_{ii}. The correlation coefficients between the estimated ith and jth parameter are

$$-1 \le \varrho_{ij} = \frac{P_{ij}}{\sqrt{P_{ii}P_{jj}}} = \frac{P_{ij}}{\sqrt{\sigma_{p_i}^2\sigma_{p_j}^2}} \le 1, \tag{11}$$

which constitute the entries of the correlation coefficient matrix $\boldsymbol{\rho}$. Since all diagonal entries of $\boldsymbol{\rho}$ are equal to 1 and $\boldsymbol{\rho}$ is symmetric, its condition number $\upsilon = \mathrm{cond}(\boldsymbol{\rho})$ is chosen as criterion for the eligibility of the respective model. At first an excitation trajectory is optimized for the identification of a basic model (see Section 3). This trajectory is used for the analysis of parameter correlation while varying model complexity, i.e., the parametrization of the friction model in passive joints. The use of the condition number allows comparable results by different dimensions (respectively to different models) of $\boldsymbol{\rho}$. The efficiency and practicability of the proposed approach has been approved by experimental results (see ref. [14] for more details).

3. Using Periodic Excitation: Implementation Issues and Data Processing

The methodology proposed by Swevers *et al.*[5,16] for the design of periodic excitation trajectories has been proved to be powerful by many researchers.[23–25] In this section the approach is extended and adapted to the case of parallel robots, since additional challenges have to be considered. Furthermore, it is emphasized on the data processing in order to improve the efficiency of periodic excitation for 6-DOF parallel manipulators.

3.1. Definition of periodic excitation for 6-DOF parallel robots

Since the dynamic model and therefore the regressor $\mathbf{\Psi}$ can be only built up by using $\boldsymbol{x}$, $\boldsymbol{v}$, and $\boldsymbol{a}$, it is recommended to define the excitation trajectories with respect to the pose of the endeffector. For each generalized coordinate corresponding to the ith element of $\boldsymbol{x}$ a respective trajectory with n_{h} harmonics is defined as

$$x_i = x_0^i + \sum_{k=1}^{n_{\mathrm{h}}}\left(\frac{\mu_k^i}{k\omega_{\mathrm{f}}}\sin(k\omega_{\mathrm{f}}t) - \frac{\nu_k^i}{k\omega_{\mathrm{f}}}\cos(k\omega_{\mathrm{f}}t)\right), \tag{12}$$

providing a proper trajectory parameter vector

$$\mathbf{\Xi}_i = \left[x_0^i,\ \mu_1^i,\ \ldots,\ \mu_{n_{\mathrm{h}}}^i,\ \nu_1^i,\ \ldots,\ \nu_{n_{\mathrm{h}}}^i\right]^{\mathrm{T}} \tag{13}$$

that contains the trajectory offset x_0^i, the trajectory coefficients $\mu_{1\ldots n_{\mathrm{h}}}^i$ and $\mu_{1\ldots n_{\mathrm{h}}}^i$ as well as the fundamental frequency ω_{f} that is common to all DOF.[5] An example of a harmonic trajectory with order $n_{\mathrm{h}} = 5$ is depicted in Fig. 1. The velocities and accelerations can be obtained in a first step by analytical derivation of Eq. (12):

$$\dot{x}_i = \sum_{k=1}^{n_{\mathrm{h}}}\left(\mu_k^i\cos(k\omega_{\mathrm{f}}t) + \nu_k^i\sin(k\omega_{\mathrm{f}}t)\right), \tag{14}$$

$$\ddot{x}_i = \sum_{k=1}^{n_{\mathrm{h}}}\left(-\mu_k^i\omega_{\mathrm{f}}k\sin(k\omega_{\mathrm{f}}t) + \nu_k^i\omega_{\mathrm{f}}k\cos(k\omega_{\mathrm{f}}t)\right). \tag{15}$$

https://doi.org/10.1017/S0263574709005682 Published online by Cambridge University Press

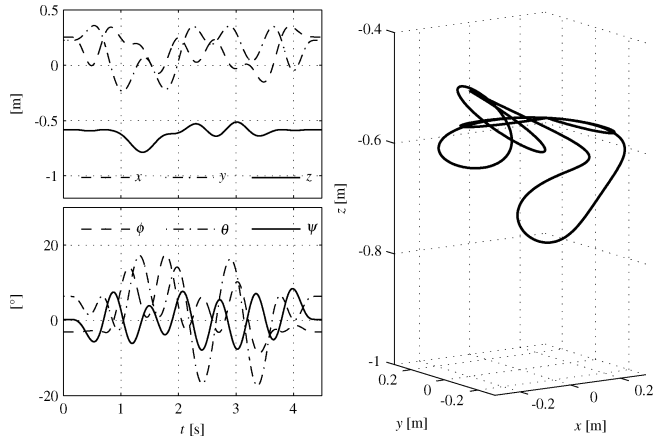

Fig. 1. Example of a periodic excitation trajectory $n_\mathrm{h} = 5$, top left: translational coordinates, bottom left: rotational coordinates, right: three-dimensional presentation.

Given the pose as $\boldsymbol{x} = [\boldsymbol{r}^\mathrm{T}\, \boldsymbol{\varphi}^\mathrm{T}]^\mathrm{T}$, with $\boldsymbol{r}$ being the cartesian position of the endeffector and $\boldsymbol{\varphi} = [\phi, \theta, \psi]^\mathrm{T}$ containing the roll pitch yaw (RPY) orientation variables, the velocities and accelerations resulting from the excitation trajectories are obtained from Eq. (14) and (15) by

$$\boldsymbol{v} = \mathcal{H}\dot{\boldsymbol{x}} \quad \text{and} \quad \boldsymbol{a} = \mathcal{H}\ddot{\boldsymbol{x}} + \dot{\mathcal{H}}\dot{\boldsymbol{x}}, \tag{16}$$

with ref. [11]

$$\mathcal{H} = \begin{bmatrix} \boldsymbol{I}_{3\times 3} & \boldsymbol{0} \\ \boldsymbol{0} & \begin{bmatrix} 1 & 0 & \sin\theta \\ 0 & \cos\psi & -\sin\psi\cos\theta \\ 0 & \sin\psi & \cos\psi\cos\theta \end{bmatrix} \end{bmatrix}.$$

Equations (12)–(16) are necessary for the trajectory optimization and for the calculation of the information matrix from the collected experimental data. The interested reader may ask, why not keep the definition of the trajectory with respect to the actuated joints and directly measurable $\boldsymbol{q}_\mathrm{a}$, as originally proposed in.[5] The answer is quite simple: if only the actuated coordinates are used, the closure constraints of the parallel manipulator have to be regarded while the optimization to provide a feasible trajectory. This demands solving additional equations with respect to a considerable number of lagrangian multipliers which increases the solution cost of the problem significantly. Furthermore, there is no possibility to avoid the numerical calculation of direct kinematics to provide the regression model. If the excitation trajectory is defined with respect to $\boldsymbol{q}_\mathrm{a}$ the direct kinematics must be performed at each iteration of the trajectory optimization and also before identification. With our proposed modification, the direct kinematics is needed only once for extracting $\boldsymbol{x}$ from the measurement of $\boldsymbol{q}_\mathrm{a}$. The related impact of data processing is discussed in the following.

3.2. Analysis of measured signals and calculated information

A necessary step in identification is the determination of the statistical properties of measured data (here the actuator positions $\boldsymbol{q}_\mathrm{a}$ and forces $\boldsymbol{Q}_\mathrm{a}$). A powerful feature of periodic excitation is the possibility of data averaging that provides a solid estimate of the measurement errors covariances.[5,16] In the classic industrial robotics and due to the decoupling effect of high gear ratios, the measurement errors are often assumed of not being cross correlated. As a result the corresponding covariance matrix is approximated by a diagonal one.[5,24,26,27] Such approach is hard to maintain for 6-DOF parallel manipulators that are characterized by a high coupling among the actuators. Therefore, the method given by Swevers *et. al* for estimating the variances of measurement errors is extended to the complete covariance matrix, i.e., $\boldsymbol{\Sigma}_{\eta\eta}$ for the output additive force measurement errors and $\boldsymbol{\Sigma}_{\delta\delta}$ for the actuator position errors $\boldsymbol{\delta}$, respectively. Averaging N_m periods of data yields for each actuator $j = 1 \ldots 6$:

$$\bar{\boldsymbol{q}}_{\mathrm{a}_j} = \frac{1}{N_\mathrm{m}} \sum_{k=1}^{N_\mathrm{m}} \boldsymbol{q}_{\mathrm{a}_{j,k}} \quad \text{and} \quad \bar{\boldsymbol{Q}}_{\mathrm{a}_j} = \frac{1}{N_\mathrm{m}} \sum_{k=1}^{N_\mathrm{m}} \boldsymbol{Q}_{\mathrm{a}_{j,k}}.$$

The generalization for the estimate of the covariance is obtained by

$$\hat{\sigma}^2_{ij}(\boldsymbol{\eta}) = \frac{1}{N}\frac{1}{N_\mathrm{m}-1} \sum_{k=1}^{N_\mathrm{m}} \left(\boldsymbol{Q}_{\mathrm{a}_{i,k}} - \bar{\boldsymbol{Q}}_{\mathrm{a}_i}\right)^\mathrm{T} \left(\boldsymbol{Q}_{\mathrm{a}_{j,k}} - \bar{\boldsymbol{Q}}_{\mathrm{a}_j}\right),$$

$$\hat{\sigma}^2_{ij}(\boldsymbol{\delta}) = \frac{1}{N}\frac{1}{N_\mathrm{m}-1} \sum_{k=1}^{N_\mathrm{m}} \left(\boldsymbol{q}_{\mathrm{a}_{i,k}} - \bar{\boldsymbol{q}}_{\mathrm{a}_i}\right)^\mathrm{T} \left(\boldsymbol{q}_{\mathrm{a}_{j,k}} - \bar{\boldsymbol{q}}_{\mathrm{a}_j}\right),$$

where $\hat{\sigma}^2_{ij}(\boldsymbol{\eta})$ and $\hat{\sigma}^2_{ij}(\boldsymbol{\delta})$ are the elements of $\boldsymbol{\Sigma}_{\eta\eta}$ and $\boldsymbol{\Sigma}_{\delta\delta}$, respectively. The validation of the provided equations for our case study PaLiDA has shown that the calculated covariance matrices deviate more or less significantly from the diagonal structure.

3.3. Data processing in the frequency domain for the calculated information

It is supposed now, the excitation experiment has been achieved on the parallel robot providing the measurements of the actuator position and forces. The necessary information about $\boldsymbol{x}$, $\boldsymbol{v}$, and $\boldsymbol{a}$ has to be extracted or filtered. The first step consists in calculating the direct kinematics to provide an estimate of the pose $\hat{\boldsymbol{x}}$. Here, the terminal condition of the numerical calculation has to be set less than the resolution of the used sensors.[11] The obtained estimate is of course noisy and has to be filtered. In their paper, Olsen and Swevers exploit the Fourier form of the excitation trajectory to achieve *implicit* frequency-domain filtering.[16] Since the trajectory harmonics correspond to the DFT transform of the signals they propose estimating the coefficients $\boldsymbol{\Xi}_i$ of the real executed trajectory. Such method would be equivalent to the selection of the first $N_\mathrm{h} + 1$ DFT coefficients. Applied to the considered case of parallel manipulators, one obtains for each DOF or each element $\hat{\boldsymbol{x}}_i$ of the pose the following set of equations (see ref. [16] for more details):

$$\hat{\boldsymbol{x}}_i = \boldsymbol{B}\ \boldsymbol{\Xi}_i, \tag{17}$$

https://doi.org/10.1017/S0263574709005682 Published online by Cambridge University Press

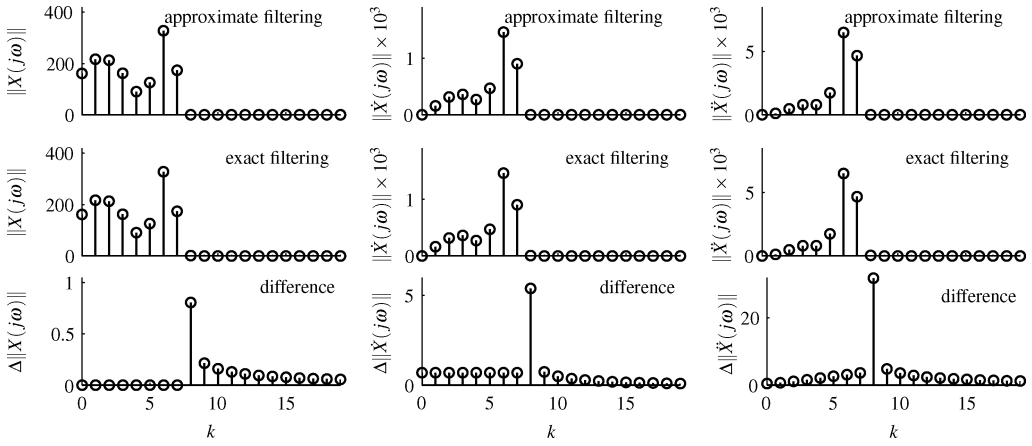

Fig. 2. Calculated and differentiated position x of the endeffector. Comparison between *top*: approximate frequency-domain filtering, *middle*: exact frequency-domain filtering and *bottom* the corresponding spectral differences.

where

$$\hat{\boldsymbol{x}}_i = [x_i(1) \cdots x_i(N)]^{\mathrm{T}}$$

$$\boldsymbol{B} = \begin{bmatrix} 1 & \frac{\mathrm{s}(t_1)}{\omega_\mathrm{f}} & \cdots & \frac{\mathrm{s}(n_\mathrm{h} t_1)}{n_\mathrm{h}\omega_\mathrm{f}} & \frac{\mathrm{c}(t_1)}{\omega_\mathrm{f}} & \cdots & \frac{\mathrm{c}(n_\mathrm{h} t_1)}{n_\mathrm{h}\omega_\mathrm{f}} \\ \vdots & \vdots & & \vdots & \vdots & & \vdots \\ 1 & \frac{\mathrm{s}(t_N)}{\omega_\mathrm{f}} & \cdots & \frac{\mathrm{s}(n_\mathrm{h} t_N)}{n_\mathrm{h}\omega_\mathrm{f}} & \frac{\mathrm{c}(t_N)}{\omega_\mathrm{f}} & \cdots & \frac{\mathrm{c}(n_\mathrm{h} t_N)}{n_\mathrm{h}\omega_\mathrm{f}} \end{bmatrix},$$

and $\mathrm{s}(t) \triangleq \sin(\omega_\mathrm{f} t)$ and $\mathrm{c}(t) \triangleq \cos(\omega_\mathrm{f} t)$. The coefficient are estimated to

$$\hat{\boldsymbol{\Xi}}_i = \left(\boldsymbol{B}^{\mathrm{T}}\boldsymbol{B}\right)^{-1} \boldsymbol{B}^{\mathrm{T}} \hat{\boldsymbol{x}}_i, \tag{18}$$

and then used to calculate the filtered data according to Eqs. (12), (14), and (15). This procedure is called *implicit* since it is actually a time-domain processing, where the transformation in the frequency domain does not occur. The equivalence to the frequency domain as claimed in ref. 16 is given only and only if the fundamental frequency ω_f of the real motion is exactly known and is exactly equal to that provided by the nominal optimized trajectory. This crucial condition is mostly fulfilled for directly measured data, as the case e.g. for encoder values. However, for the considered case of calculated signals this is not the case. Due to the terminal condition of the numerical direct kinematics the period of the calculated motion $\hat{\boldsymbol{x}}$ is not exactly the same as the nominal one. Furthermore, it varies from repetition to repetition depending on when the numerical procedure has stopped. As a result, applying Eq. (18) will lead to leakage errors. Therefore, we recommend the explicit calculation of the DFT transform $\hat{\boldsymbol{x}}_i \rightarrow \hat{X}_i(j\omega)$. Afterwards the spectrum is filtered by a frequency-domain low-pass filter. Ideal filtering can be achieved by means of a rectangular window with a desirable cutoff frequency f_c. The latter may be chosen (but is not limited to) to correspond the nominal fundamental frequency: $f_c \triangleq n_\mathrm{h}\omega_\mathrm{f}/2\pi$. The windowed and filtered spectrum $X_i(j\omega)$ is multiplied twice by $j\omega$

$$\dot{X}_i(j\omega) = j\omega X_i(j\omega),$$
$$\ddot{X}_i(j\omega) = -\omega^2 X_i(j\omega).$$

Transforming back to the time domain yields the filtered signals $\dot{\hat{\boldsymbol{x}}}_i = \mathrm{DFT}^{-1}(\dot{X}_i(j\omega))$ and $\ddot{\hat{\boldsymbol{x}}}_i = \mathrm{DFT}^{-1}(\ddot{X}_i(j\omega))$. The pose estimate is also updated according to $\hat{\boldsymbol{x}}_i = \mathrm{DFT}^{-1}(X_i(j\omega))$. The filtered estimates of the velocities and accelerations of the endeffector are provided by using Eq. (16)

$$\hat{\boldsymbol{v}} = \boldsymbol{\mathcal{H}}(\hat{\boldsymbol{x}})\dot{\hat{\boldsymbol{x}}} \quad \text{and} \quad \hat{\boldsymbol{a}} = \boldsymbol{\mathcal{H}}(\hat{\boldsymbol{x}})\ddot{\hat{\boldsymbol{x}}} + \dot{\boldsymbol{\mathcal{H}}}(\hat{\boldsymbol{x}})\dot{\hat{\boldsymbol{x}}}.$$

Additional to its simplicity, there are many advantages of an *explicit* or strictly frequency-domain data processing. First, it is possible to achieve ideal and exact low-pass filtering that guarantees the rejection of all frequency components beyond f_c. Such feature is of course due to the periodic excitation approach. Second, no leakage effects are introduced even in the case of biased ω_f. This property is demonstrated in Fig. 2 by comparing the spectra of x_1, $\dot{x}_1$ and $\ddot{x}_2$ resulting from the approximate Eq. (18) and from the here proposed exact frequency-domain processing, respectively. The example is given for experimental data using a trajectory with $n_\mathrm{h} = 7$. The used cutoff corresponds to the nominal fundamental frequency. As it can be noticed there exists spectral difference for all frequency components. Since it is sure that the exact frequency-domain approach provides zero signals beyond the $n_\mathrm{h} + 1$ frequency component, the difference is clearly caused by leakage. The latter is due to the mistuning of ω_f introduced by the direct kinematics. The bias $\delta\omega_\mathrm{f}$ corresponds to the constant difference in $\|\dot{X}(j\omega)\|$ beneath the cutoff. By using the proposed explicit frequency-domain processing, the consideration of the realistic case, when the measured trajectory contains more than the nominal n_h harmonics is straightforward. Adjusting the desired cutoff is then sufficient. This flexibility in data processing will be exploited later to provide a new implementation of the maximum-likelihood approach that allows for tuning automatically the cutoff frequency f_c. Finally, it is worthy to mention that there is no need to filter the actuator forces since the respective noise does not affect the regressor and is additive to the output. The linear estimation techniques are adequate for such case. All our experiments have shown that filtering the actuator forces yields higher biased estimates.[13] The main reason is the filtering of discontinuous friction dynamics in

https://doi.org/10.1017/S0263574709005682 Published online by Cambridge University Press

the measurement vector $\boldsymbol{\Gamma}$, such that a mismatch is introduced between the estimation equation and the assumed dynamics model.

At this stage, information on $\boldsymbol{x}$, $\boldsymbol{v}$, and $\boldsymbol{a}$ can be calculated accurately. Furthermore, statistical properties of all necessary signals are provided by full covariance matrices. A disturbance-poor information matrix that can be additionally used to determine best identifiable model structure as suggested in Section 2. The identification is achieved by Eq. (9) to obtain the parameter estimates. Before showing the results, the influence of the experiment design should be first discussed.

4. Optimal Input Experiment Design

The optimal experiment design is the methodology to determine an experiment for collecting N measurements in order to achieve "*best*" identification results. This is equivalent to the generation of optimal excitation trajectories $\mathcal{T}(\boldsymbol{\Xi})$ by adjusting the trajectory parameter vector

$$\boldsymbol{\Xi} = \left[\boldsymbol{\Xi}_1^{\mathrm{T}}, \ldots \boldsymbol{\Xi}_6^{\mathrm{T}}, \omega_{\mathrm{f}} \right]^{\mathrm{T}}, \tag{19}$$

containing the coefficients of all DOFs and the fundamental pulsation and having the dimension $\dim(\boldsymbol{\Xi}) = 6 \cdot (2\,n_{\mathrm{f}} + 1) + 1 = 12n_{\mathrm{f}} + 7$. The design consists in a constrained nonlinear optimization.[5,18] The required constraints are expressed with respect to the actuation variables

$$\begin{array}{l} \boldsymbol{q}_{\mathrm{a}}^{\min} \le \boldsymbol{q}_{\mathrm{a}}(t, \boldsymbol{\Xi}) \le \boldsymbol{q}_{\mathrm{a}}^{\max}, \\ \dot{\boldsymbol{q}}_{\mathrm{a}}^{\min} \le \dot{\boldsymbol{q}}_{\mathrm{a}}(t, \boldsymbol{\Xi}) \le \dot{\boldsymbol{q}}_{\mathrm{a}}^{\max}, \\ \ddot{\boldsymbol{q}}_{\mathrm{a}}^{\min} \le \ddot{\boldsymbol{q}}_{\mathrm{a}}(t, \boldsymbol{\Xi}) \le \ddot{\boldsymbol{q}}_{\mathrm{a}}^{\max}, \end{array} \quad \forall\, \boldsymbol{\Xi} \text{ and } t \in [0, T_{\mathrm{f}}], \tag{20}$$

to account for actuator limitation and therefore indirectly for workspace constraints and dynamics capabilities of the manipulator. The inverse kinematics has to be performed while the optimization, which does not introduce any significant computational cost due to its simplicity. Of course, it is possible to express the constraints *ad hoc* with respect to $\boldsymbol{x}$, $\boldsymbol{v}$, and $\boldsymbol{a}$. It depends on the considered manipulator, whether such approach is preferable or not, since it results in different constraints than Eq. (20), which can accelerate the convergence of the optimization process. The optimization or the experiment design criterion should contribute to the reduction of parameter uncertainty. A recent overview on optimal input design is given in ref. [28] as well as in.[19,29] It is focused in the following on the reputed approaches in robotics that chose the condition number of $\boldsymbol{\Psi}$ as a minimization criteria:[4,13–25]

$$\boldsymbol{\Xi}^{(\mathrm{de})} = \arg \left\{ \min_{\boldsymbol{\Xi}} \left(\mathrm{cond}(\boldsymbol{\Psi}(\boldsymbol{\Xi})) \right) \right\}. \tag{21}$$

A direct relationship to parameter uncertainty can be derived under the assumption of noise-free regressor. Using the condition number aims the orthogonalization of the estimation confidence ellipsoid and can be therefore considered as a kind of modified C-optimal design.[29] In ref. [5] the minimization of the condition number was called *deterministic* design since it assumes a deterministic noise-free regressor. This terminology is kept here. In contrast, *statistical* or D-optimal design accounts for measurement disturbances and aims increasing the volume of the asymptotic confidence ellipsoid for the parameter estimates,[18,19,28] which is equivalent to the determinant of $\boldsymbol{P}$

$$\boldsymbol{\Xi}^{(\mathrm{s})} = \arg \left\{ \min_{\boldsymbol{\Xi}} \left(-\ln \det \left(\boldsymbol{\Psi}^{\mathrm{T}} \boldsymbol{\Sigma}_{\eta\eta}^{-1} \boldsymbol{\Psi} \right) \right) \right\}. \tag{22}$$

No matter which criterion is used, the optimization is mostly a nonconvex one and the obtained results will not correspond to the global minimum. This is however not critical since for experimental identification just a sufficiently good excitation trajectory is needed. The most important difference between the discussed criteria is that the statistical design is independent from any nonsingular scaling or reparametrization that does not depend on the experiment itself.[19] This is not the case for the method using the condition number that is already a scaled value. Our experience demonstrated that the scaled property leads to slower but a more robust optimization process. In contrast, optimizing the confidence ellipsoid volume is quicker but get often stuck in local minima that violate the constraints. For the statistical design trial-and-error steps are eventually necessary. In the experimental results section, the influence of both design methodologies on the obtained parameter estimates is presented. The trajectory depicted in Fig. 1 is optimized according to the statistical design and is used for experimental investigations in the next sections.

5. On the Use of Maximum-Likelihood Estimator for Parallel Robots

More general to the discussed linear estimation is the maximum-likelihood approach.[19] Olsen has proposed the direct application of the maximum-likelihood estimates to serial-link robots.[16,24,27] To reduce the computational burden he proposed the elegant analytical linearization of the complete dynamics and related constraints with respect to measured (or calculated) observations. Unfortunately, such approach won't work for the case of 6-DOF parallel manipulator. This is not only due to the highly more complex dynamics but mostly to the lack of a final closed form with respect to the actuation variables. The presence of the numerically obtainable $\boldsymbol{J}$ in Eq. (7) inhibits the possibility of building the gradient or partial derivatives of the dynamics to apply maximum-likelihood estimate like suggested in ref. [27].

A practical implementation consists in considering only the measured variables of position and actuation forces. Giving the measurement errors $\boldsymbol{\delta}(k)$ of the actuator position and the output additive disturbances $\boldsymbol{\eta}(k)$ with respective covariances $\boldsymbol{\Sigma}_{\delta\delta}$ and $\boldsymbol{\Sigma}_{\eta\eta}$ a maximum-likelihood expression ca be derived as follows

$$\hat{\boldsymbol{p}}_{\mathrm{ML}} = \arg \left\{ \min_{\boldsymbol{p}} \left(\frac{1}{2} \sum_{k=1}^{N} \left(\boldsymbol{\delta}^{\mathrm{T}}(k) \boldsymbol{\Sigma}_{\delta\delta}^{-1} \boldsymbol{\delta}(k) + \boldsymbol{\eta}^{\mathrm{T}}(k, \boldsymbol{p}) \boldsymbol{\Sigma}_{\eta\eta}^{-1} \boldsymbol{\eta}(k, \boldsymbol{p}) \right) \right) \right\}. \tag{23}$$

https://doi.org/10.1017/S0263574709005682 Published online by Cambridge University Press

Since the real values are unknown, the considered measurement errors present only an estimate that has been obtained by data processing. The latter should be then involved in Eq. (23) by extending the parameter vector to be estimated

$$\left[\hat{\boldsymbol{p}}_{\mathrm{ML}}^{\mathrm{T}}\ \hat{\boldsymbol{p}}_{\mathrm{z}}^{\mathrm{T}}\right]^{\mathrm{T}} = \arg\left\{\min_{\boldsymbol{p}}\left(\frac{1}{2}\sum_{k=1}^{N}\left(\boldsymbol{\delta}^{\mathrm{T}}(k,\boldsymbol{p}_{\mathrm{z}})\boldsymbol{\Sigma}_{\delta\delta}^{-1}\boldsymbol{\delta}(k,\boldsymbol{p}_{\mathrm{z}})\right.\right.\right.$$
$$\left.\left.\left.+\boldsymbol{\eta}^{\mathrm{T}}(k,\boldsymbol{p},\boldsymbol{p}_{\mathrm{z}})\boldsymbol{\Sigma}_{\eta\eta}^{-1}\boldsymbol{\eta}(k,\boldsymbol{p},\boldsymbol{p}_{\mathrm{z}})\right)\right)\right\}, \quad (24)$$

where $\boldsymbol{p}_z$ accounts for data processing parameters. They depend on the used approach for filtering or calculating the necessary information. The proposed implementation is coherent with the approach proposed by Swevers *et al.*[5] that can be derived from Eq. (24) by simply setting $\boldsymbol{p}_z \triangleq \hat{\boldsymbol{\Xi}} - \{\omega_{\mathrm{f}}\}$ and yields the simultaneous estimation of model parameters and the coefficients of the real executed trajectory by the manipulator. In contrast to such method and as a consequence of the proposed strict frequency domain filtering we suggest the following choice

$$\boldsymbol{p}_z \triangleq f_c$$

that yields the automatic tuning of the filter cutoff to the relevant bandwidth of the measurements. This novel proposition has several advantages. First, it helps enhancing the computational efficiency of the maximum-likelihood procedure considerably. The dimension of the nonlinear optimization is reduced by $12n_{\mathrm{h}} + 6$ for any excitation trajectory with n_{h} harmonics, which is considerable. Second, it adjusts automatically and without any additional effort the information bandwidth. That is, in the case when the real trajectory contains relevant frequencies beyond the nominal fundamental one. In the alternative approach,[5] many optimization trials are necessary to determine the optimal dimension of $\boldsymbol{p}_z$.[5,16] It is rather to notice that in the case when $\boldsymbol{\delta} \approx \mathbf{0}$ the solution of Eq. (24) corresponds exactly to the GM estimates. This was observed in our experimental studies for some trajectories, where the remaining disturbances of the filtered actor positions were negligible.

6. Experimental Results

In this section the proposed strategy of dynamics identification for a 6-DOF parallel robot is substantiated with experimental results achieved on the hexapod PaLiDA (see Fig. 3 and ref. 30). The parallel robot has been designed to be a mixture between a high-speed manipulator and a tool machine. The application area covers fast handling and light cutting machining tasks with low-process forces. To achieve high-manoeuvrability and high-dynamics ability, PaLiDA has been equipped with fast electromagnetic direct drives.[30] These drives lacks however of accurate measurement sensors (only internal hall sensors are used), such that model-based control is necessary to achieve satisfactorily high-tracking accuracy. Fortunately, the study of the measurement noise of position ($\boldsymbol{\delta}$) and current (proportional to $\boldsymbol{\eta}$) demonstrated their gaussian and zero-mean quality. Thus, the assumptions

Fig. 3. Case study: Hexapod PaLiDA. Left: presentation in the Hannover industrial fair, 2001. Right: CAD model.

Table I. Rigid-body and friction model parameters for the parallel robot PaLiDA.

Rigid body	Friction
$p_1 = I_{zz_1} + I_{yy_2} + I_{zz_3}$ [kg m^2]	r_α [N]
$p_2 = I_{xx_2} + I_{xx_3} - I_{yy_2} - I_{zz_3}$ [kg m^2]	r_β [N]
$p_3 = I_{zz_2} + I_{yy_3}$ [kg m^2]	r_1 [N]
$p_4 = s_{y_2}$ [kg m]	r_2 [N]
$p_5 = s_{y_3}$ [kg m]	r_3 [N]
$p_6 = I_{xx_E} + m_3 \sum_{j=1}^{6}(r_{By_j}^2 + r_{Bz_j}^2)$ [kg m^2]	r_4 [N]
$p_7 = I_{yy_E} + m_3 \sum_{j=1}^{6}(r_{Bx_j}^2 + r_{Bz_j}^2)$ [kg m^2]	r_5 [N]
$p_8 = I_{zz_E} + m_3 \sum_{j=1}^{6}(r_{Bx_j}^2 + r_{By_j}^2)$ [kg m^2]	r_6 [N]
$p_9 = s_{z_E} + m_3 \sum_{j=1}^{6} r_{Bz_j}$ [kg m]	v_1 [Ns/m]
$p_{10} = m_E + 6m_3$ [kg]	v_2 [Ns/m]
	v_3 [Ns/m]
	v_4 [Ns/m]
	v_5 [Ns/m]
	v_6 [Ns/m]

on applying the above proposed estimation techniques are fulfilled.

The dynamics model of the robot consists in 10 rigid-body minimal parameters and 14 friction coefficients (see Table I). Its long and place consuming derivation is omitted here. The interested reader is referred to our former publications.[14,15] For space reasons we will present in the following three important experimental results: the effect of data processing on the prediction quality of the model, the effect of experiment design on the accuracy of the parameter estimates and the influence of the estimator on the identification results.

First, three identified models are considered that were obtained from the same trajectory but according to different data processing. The first one results from rough and nonfiltered data. For the second, the measurements of the actuator lengths were filtered in the time domain by a low-pass filter as suggested e.g. in refs. [7, 17]. The third model has been identified according to the frequency domain method, as proposed in Section 3.3. The validation of the models on a circular bench-mark trajectory, which was not used for identification, is depicted in Fig. 4. The frequency-domain processing yields the best prediction quality corresponding to the smallest error variance σ^2. Time-domain filtering is not accurate enough to extract all information at the relevant frequencies.

Another important result is related to the experiment design. It has been suggested earlier that from the theoretical

https://doi.org/10.1017/S0263574709005682 Published online by Cambridge University Press

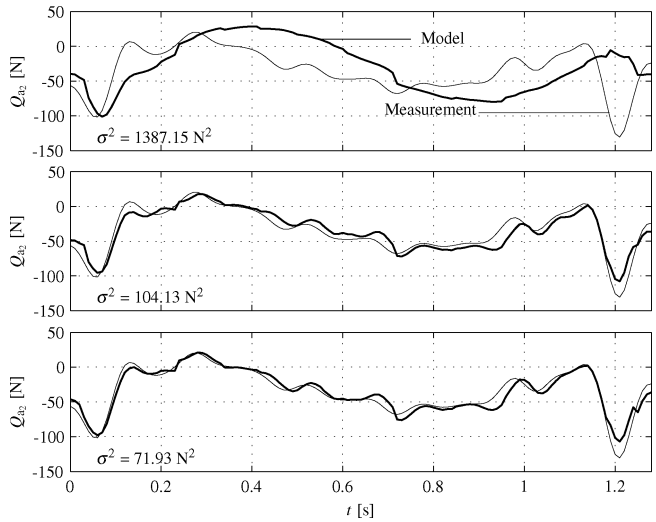

Fig. 4. Prediction accuracy of three different models for an arbitrarily chosen actuator. Top: by using rough data, middle: by using time-domain filtering, bottom: by using frequency-domain filtering.

Table II. Comparison of the identified parameter corresponding to different estimators.

p_k	$\hat{p}_{\mathrm{GM}}$	$\hat{p}_{\mathrm{ML}}$	*a priori*
p_1 [kg m^2]	−0.0447	−0.0444	0.0074
p_2 [kg m^2]	1.0892	1.0915	0.9439
p_3 [kg m^2]	1.0077	1.0106	0.9458
p_4 [kg m]	0.5995	0.6029	0.6201
p_5 [kg m]	−1.2885	−1.2898	−1.2295
p_6 [kg m^2]	0.3078	0.3084	0.2878
p_7 [kg m^2]	0.3021	0.3018	0.2878
p_8 [kg m^2]	0.1176	0.1173	0.1217
p_9 [kg m]	1.8896	1.8874	1.9012
p_{10} [kg]	16.3081	16.2966	16.1920
r_α [Nm]	0.5756	0.5593	–
r_β [Nm]	0.9195	0.9339	–
r_1 [N]	11.9772	12.1195	–
r_2 [N]	4.8071	5.1917	–
r_3 [N]	20.1528	20.1773	–
r_4 [N]	5.1518	5.4981	–
r_5 [N]	1.5857	1.7191	–
r_6 [N]	5.0057	4.9622	–
v_1 [Ns/m]	16.8771	16.7115	–
v_2 [Ns/m]	16.7406	16.1764	–
v_3 [Ns/m]	6.3408	6.2864	–
v_4 [Ns/m]	23.1662	22.6607	–
v_5 [Ns/m]	26.4675	26.3370	–
v_6 [Ns/m]	22.8053	22.8194	–
f_c [Hz]	1.6182	1.6195	–

point of view the statistical design of the excitation trajectories Eq. (22) yields parameter estimates with less uncertainty. We achieve the experimental proof by using the same set of initial parameters to optimize two excitation trajectories of the fifth order according to Eqs. (21) and (22), respectively. To obtain statistically sensible results each trajectory was measured and evaluated 100 times. The identification procedure was achieved for each measurement trial to obtain parameter sets corresponding to each design approach. The resulting normal distributions estimated from the identified parameters over the trials can be compared as illustrated exemplarily for the rigid-body parameters (see Fig. 5). It is obvious that the trajectory corresponding to the statistical criterion yields smaller standard deviations, which means smaller estimation uncertainty. This was observed for almost all parameters.

The same statistically optimized trajectory is used to compare the estimates resulting from the Markov nd the proposed maximum-likelihood approach (Table II). Additionally, a priori values of the rigid-body model ar given, which do not present the true parameters, since they were calculated by using CAD-Data. The estimate of the appropriate filter-cutoff f_c is also presented, is only obtainable by using the proposed maximum-likelihood approach (Eq. (24)). It can be noticed that f_c was very finely tuned by an amount that is much smaller than an additional harmonic corresponding to the fundamental frequency. This tuning is very hard to obtain via trial-and-error procedures. To be fair, in our experiments, the use of the maximum-likelihood estimation did not lead to a sensible improvement of the model prediction quality. Our proposed method is therefore meant to be an additional idea that is at least much more computationally efficient than

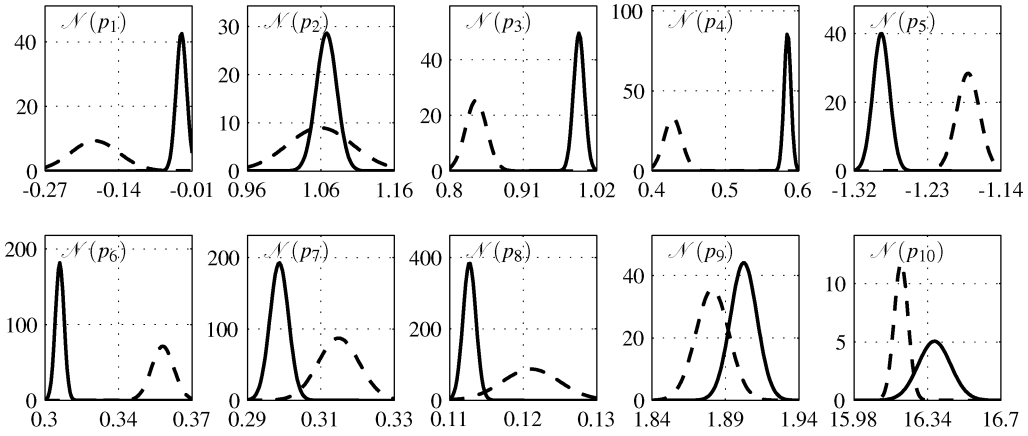

Fig. 5. Estimated normal distribution $\mathcal{N}(\hat{\boldsymbol{p}})$ for parameter resulting from deterministic design $\hat{\boldsymbol{p}}^{(\mathrm{de})}$ (dashed line) and parameter resulting from statistical design $\hat{\boldsymbol{p}}^{(\mathrm{s})}$ (continuous line). All x- and y-axis relate to the parameter value, and to the corresponding distribution density.

https://doi.org/10.1017/S0263574709005682 Published online by Cambridge University Press

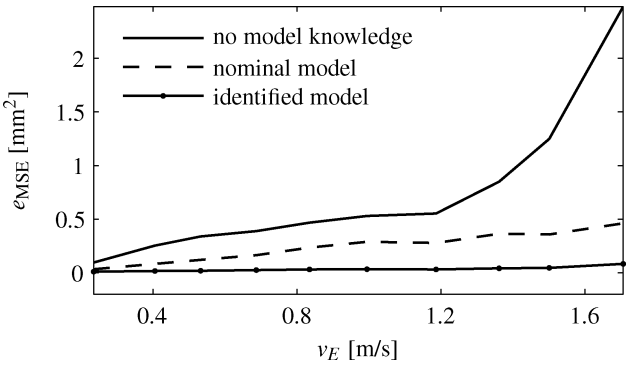

Fig. 6. Influence of model accuracy on the improvement of tracking quality: using different feedforward models with underlaying proportional integral derivative (PID) control.

other approaches.[5,16] It may also yields higher improvement in the case of other systems or measuring conditions. In our case the Markov estimate was the best compromise in terms of model prediction quality and computational effort. The study of parameter bias is however not quite simple because the real values are missing. This is especially the case for friction parameters that vary depending on operating conditions. Furthermore and since all measurement are carried out in closed loop, the dynamics of the controller affects the resulting estimates, such that all parameter sets are expected to be more or less biased.[18] The latter issue is however less critical for control purposes, since the model prediction quality is more interesting than the exact parameter values. A related experiment shows the important role of identification for improving control accuracy. The parameter set $\hat{\boldsymbol{p}}_{GM}$ provided by the Markov estimate for the inverse model is used as a feedforward compensator. The validation motion of Fig. 4 is executed at different velocities while collecting the mean-squares tracking error e_{MSE} of all actuators over the trials. The results are depicted by Fig. 6. It is clear that the identification contributes enormously to the improvement of control performance. The tracking accuracy is very poor when no model knowledge is used. The nominal model with a priori parameters is also unable to achieve high-quality tracking. A dependency of the errors on the endeffector velocity is still noticeable. Only accurately identified model allows keeping good tracking performance over the investigated range of dynamics.

7. Conclusions

The aim of this paper is to give a self-contained approach for the identification of the dynamics model of 6-DOF parallel robots. The structural properties of such systems were stressed to motivate the developed methodologies and the proposed extensions of known approaches. The paper proves that periodic excitation is a powerful method for parallel robots. Due to the actuator coupling, the consideration of cross-covariances in the measurement becomes necessary. Furthermore, the need of calculating the direct kinematics suggests an explicit or strict frequency-domain filtering of the measurement to avoid leakage effects. Extensive experiments have demonstrated that the excitation trajectories should be optimized in a statistical frame work to provide less parameter uncertainty, especially when used in combination with the Markov estimate. Additionally, a new and computationally highly efficient implementation of the maximum-likelihood estimation is provided. Here, the cutoff-frequency of the data filtering can be optimized automatically.

References

1. C. H. An, C. G. Atkeson and J. M. Hollerbach, "Model-Based Control of a Robot Manipulator," **In**: *The MIT Press Series in Artificial Intelligence* (The MIT Press, 1988).
2. K. Kozlowski, "*Modelling and Identification in Robotics*," In: *Advances in Industrial Control* (Springer-Verlag, 1998).
3. W. Khalil and E. Dombre, *Modeling, Identification and Control of Robots* (Hermes, London, UK, 2002).
4. M. Gautier and W. Khalil, "Exciting trajectories for the identification of base inertial parameters of robots," *Int. J. Robot. Res.* **11**(4), 362–375 (1992).
5. J. Swevers, C. Gansemann, D. Tükel, J. D. Schutter and H. V. Brussel, "Optimal robot excitation and identification," *IEEE Trans. Robot. Autom.* **13**(5), 730–740 (1997).
6. S. Guegan, W. Khalil and P. Lemoine, "Identification of the Dynamic Parameters of the Orthoglide," *Proceedings of the 2003 IEEE International Conference on Robotics and Automation*, Taipei, Taiwan (2003) pp. 3272–3277.
7. A. Vivas *et al.*, "Experimental Dynamic Identification of a Fully Parallel Robot," *Proceedings of the 2003 IEEE International Conference on Robotics and Automation*, Taipei, Taiwan (2003), pp. 3278–3283.
8. N. Ramdani and P. Poignet, "Experimental Parallel Robot Dynamic Model Evaluation with set Membership Estimation," *Proceedings of the 14th IFAC Symposium on System Identification*, Newcastle, Australia (2006).
9. N. Farhat, V. Mata, À. lvaro Page and F. Valero, "Identification of dynamic parameters of a 3-dof rps parallel manipulator," *Mech. Mach. Theory* **43**(1), 1–17 (2008).
10. J.-P. Merlet, "Jacobian, manipulability, condition number, and accuracy of parallel robots," *J. Mech. Des.* **128**(1), 199–206 (2006).
11. J.-P. Merlet, "*Parallel Robots*," **In**: *Solid Mechanics and its Applications* (Kluwer Academic Publishers, 2000).
12. H. Abdellatif and B. Heimann, *Industrial Robotics: Theory, Modeling and Control* (Pro-Literatur Verlag, 2007) pp. 523–556.
13. H. Abdellatif, F. Benimeli, B. Heimann and M. Grotjahn, "Direct Identification of Dynamic Parameters for Parallel Manipulators," *Proceedings of the International Conference on Mechatronics and Robotics 2004, MechRob2004*, Aachen, Germany (2004) pp. 999–1005.
14. H. Abdellatif, B. Heimann, O. Hornung and M. Grotjahn, "Identification and Appropriate Parametrization of Parallel Robot Dynamic Models by Using Estimation Statistical Properties," *Proceedings of the 2005 IEEE/RSJ International Conference on Intelligent Robots and Systems, IROS2005*, Edmonton, Canada (2005) pp. 444–449.
15. H. Abdellatif, M. Grotjahn and B. Heimann, "High Efficient Dynamics Calculation Approach for Computed-Force Control of Robots with Parallel Structures," *Proceedings of the 44th IEEE Conference on Decision and Control and the 2005 European Control Conference, CDC-ECC05*, Seville, Spain (2005) pp. 2024–2029.
16. M. M. Olsen, J. Swevers and W. Verdonck, "Maximum likelihood identification of a dynamic robot model: Implementation issues," *Int. J. Robot. Res.* **21**(2), 89–96 (2002).
17. M. Gautier and P. Poignet, "Extended kalman filtering and weighted least squares dynamic identification of robot," *Control Eng. Practice* **9**(12), 1361–1372 (2001).

https://doi.org/10.1017/S0263574709005682 Published online by Cambridge University Press

18. L. Ljung, *System Identification: Theory for the User*, 2nd ed. (Prentice-Hall, Upper Saddle Hall, NJ, 1999).
19. E. Walter and L. Pronzato, *Identification of Parametric Models form Experimental Data* (Springer-Verlag, London, UK: 1997).
20. K. Harib and K. Srinivasan, "Kinematic and dynamics analysis of stewart platform-based machine tool structures," *Robotica* **21**, 541–554 (2003).
21. H. Abdellatif and B. Heimann, "On Compensation of Passive Joint Friction in Robotic Manipulators: Modeling, Detection and Identification," *Proceedings of the 2006 IEEE International Conference on Control Applications, CCA2006*, Munich, Germany (2006) pp. 2510–2515.
22. W. Khalil and S. D. Guegan, "Inverse and direct dynamics modeling of gough-stewart robots," *IEEE Trans. Robot.* **20**(4), 754–762 (2004).
23. D. Kostic, B. de Jager, M. Steinbuch and R. Hensen, "Modeling and identification for high-performance robot control: An rrr-robotic arm case study," *IEEE Trans. Control Syst. Technol.* **12**(6), 904–919 (2004).
24. B. Bona and A. Curatella, "Identification of Industrial Robot Parameters for Advanced Model-Based Controllers Design," *Proceedings of the 2005 IEEE International Conference on Robotics and Automation* Barcelona, Spain (2005) pp. 1693–1698.
25. V. Mata, F. Benimeli, N. Farhat and A. Valera, "Dynamic parameter identification in industrial robots considering physical feasibility," *Adv. Robot.* **19**(1), 101–119 (2005).
26. J.-M. Renders, E. Rossignol, M. Becquet and R. Hanus, "Kinematic calibration and geometrical parameter identification for robots," *IEEE Trans. Robot. Autom.* **7**(6), 721–432 (1991).
27. M. M. Olsen and H. G. Petersen, "A new method for estimating parameters of a dynamic robot model," *IEEE Trans. Robot. Autom.* **17**(1), 95–100 (2001).
28. M. Gevers, "Identification for control: From the early achievements to the revival of experiment design," *Eur. J. Control* **11**(4–5), 335–352 (2005).
29. A. F. Emery and A. V. Nenarokomov, "Optimal experiment design," *Meas. Sci. Technol.* **49**(9), 864–876 (1998).
30. B. Denkena, B. Heimann, H. Abdellatif and C. Holz, "Design, Modeling and Advanced Control of the Innovative Parallel Manipulator Palida," *Proceedings of the 2005 IEEE/ASME International Conference on Advanced Intelligent Mechatronics, AIM2005* Monterrey, CA (2005) pp. 632–637.

https://doi.org/10.1017/S0263574709005682 Published online by Cambridge University Press